Evaluation of Genetically Encoded Chemical Tags as Orthogonal Fluorophore Labeling Tools for Single-Molecule FRET Applications

ARTICLE *in* THE JOURNAL OF PHYSICAL CHEMISTRY B · MAY 2015

Impact Factor: 3.3 · DOI: 10.1021/acs.jpcb.5b03584 · Source: PubMed

6 AUTHORS, INCLUDING:

Yuji Ishitsuka
University of Illinois, Urbana-Champaign
35 PUBLICATIONS **1,043** CITATIONS
SEE PROFILE

Naghmeh Azadfar
University of Tuebingen
5 PUBLICATIONS **156** CITATIONS
SEE PROFILE

Andrei Yu Kobitski
Karlsruhe Institute of Technology
54 PUBLICATIONS **935** CITATIONS
SEE PROFILE

THE JOURNAL OF PHYSICAL CHEMISTRY B

Article

pubs.acs.org/JPCB

Evaluation of Genetically Encoded Chemical Tags as Orthogonal Fluorophore Labeling Tools for Single-Molecule FRET Applications

Yuji Ishitsuka,[†,‡] Naghmeh Azadfar,[†,‡,¶] Andrei Yu. Kobitski,[†] Karin Nienhaus,[†] Nils Johnsson,[§] and G. Ulrich Nienhaus*[,†,∥,⊥]

[†]Institute of Applied Physics, Karlsruhe Institute of Technology (KIT), Wolfgang-Gaede-Strasse 1, 76131 Karlsruhe, Germany

[§]Institute of Molecular Genetics and Cell Biology, Ulm University, James Franck Ring N27, 89081 Ulm, Germany

[∥]Institute of Toxicology and Genetics, Karlsruhe Institute of Technology (KIT), Hermann-von-Helmholtz-Platz 1, 76344 Eggenstein-Leopoldshafen, Germany

[⊥]Department of Physics, University of Illinois at Urbana−Champaign, 1110 West Green Street, Urbana, Illinois 61801, United States

Supporting Information

ABSTRACT: Fluorescence resonance energy transfer (FRET) is a superb technique for measuring conformational changes of proteins on the single molecule level (smFRET) in real time. It requires introducing a donor and acceptor fluorophore pair at specific locations on the protein molecule of interest, which has often been a challenging task. By using two different self-labeling chemical tags, such as Halo-, TMP-, SNAP- and CLIP-tags, orthogonal labeling may be achieved rapidly and reliably. However, these comparatively large tags add extra distance and flexibility between the desired labeling location on the protein and the fluorophore position, which may affect the results. To systematically characterize chemical tags for smFRET measurement applications, we took the SNAP-tag/CLIP-tag combination as a model system and fused a flexible unstructured peptide, rigid polyproline peptides of various lengths, and the calcium sensor protein calmodulin between the tags. We could reliably identify length variations as small as four residues in the polyproline peptide. In the calmodulin system, the added length introduced by these tags was even beneficial for revealing subtle conformational changes upon variation of the buffer conditions. This approach opens up new possibilities for studying conformational dynamics, especially in large protein systems that are difficult to specifically conjugate with fluorophores.

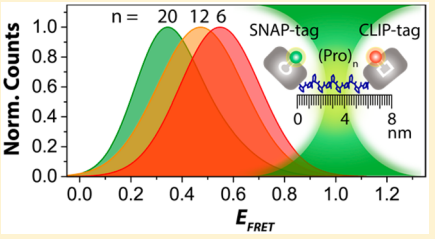

INTRODUCTION

Fluorescence resonance energy transfer (FRET) is a non-radiative energy transfer process between the transition dipoles of a fluorescent donor molecule and an acceptor molecule occurring over distances of up to 100 Å. As described by Förster in 1946, the energy transfer efficiency is proportional to the inverse sixth power of the distance between the chromophores.[1,2] Due to this strong distance dependence, FRET has often been called a spectroscopic ruler.[3]

Because the FRET sensitivity range is comparable to the typical dimensions of biological macromolecules, FRET has been utilized extensively to study biomolecular interactions and conformational changes. Studying the dynamics of single molecules using FRET is especially revealing because certain properties of the sample, such as the presence of subpopulations or heterogeneity of kinetic parameters, can be uncovered that would normally be masked by ensemble averaging.[4−7]

Any single molecule FRET (smFRET) measurement requires labeling of the biomolecule(s) of interest with a pair of fluorophores. The specific labeling of nucleic acids has become routine practice; they may even be purchased in the labeled form. In contrast, there is no one-fits-all procedure capable of achieving site-specific labeling of proteins. A common approach to attach a fluorescent label involves a reaction between an *N*-hydroxysuccinimidyl (NHS) ester-functionalized dye and a primary amine moiety on the protein, such as the N-terminal amino group or a lysine side chain. However, because of the typically large number of lysine residues on the protein surface, the conjugation will not be site-specific, and thus, both the number of dyes attached to a single protein and the individual attachment site(s) will vary. For the labeling specificity to be increased, the dyes may be attached to the less abundant cysteines (e.g., by thiol-maleimide chemistry). Often, proteins have only a few (if any) exposed cysteines, and in addition, there are clever blocking methodologies available to control the number of reactive cysteines.[8] Still, site-specific labeling of a particular cysteine may become complicated when dealing with multiple cysteines, which is likely the case with larger proteins. Alternative strategies that allow orthogonal labeling of proteins include the incorporation of unnatural amino acids,[9−12] the addition of short peptide tags recognizable by specific chemicals or enzymes (e.g., His-,[13] aldehyde-,[14,15] tetracysteine-,[16] TGase-,[17] and coiled-coil-[18] tags), the

Received: April 14, 2015
Revised: May 15, 2015

DOI: 10.1021/acs.jpcb.5b03584
J. Phys. Chem. B XXXX, XXX, XXX−XXX

utilization of protein ligases[19] (e.g., intein[20] and sortase[21,22]), and the fusion of protein domains that function as self-labeling chemical tags (e.g., Halo-,[23] TMP-,[24,25] SNAP-, and CLIP-[26,27] tags) to the protein of interest. These self-labeling protein tags are 18−33 kDa in size and engineered to selectively bind their target ligand.

The SNAP- and CLIP-tags are genetically encoded chemical tags derived from the 20 kDa DNA repair protein human O^6-alkylguanine-DNA-alkyltransferase (hAGT).[26,27] They catalyze the covalent attachment of O^6-benzylguanine (BG) to the SNAP-tag or O^6-benzylcytosine (BC) to the CLIP-tag of a reactive cysteine residue (Cys145) located close to their geometrical center.[26] Because there is no additional cofactor necessary for the reaction between the BG-/BC-functionalized ligand and the respective tag, the labeling reaction will proceed in vitro (i.e., by using purified protein samples) and also in vivo (i.e., within living cells) by using membrane-permeable ligands (Figure 1). To date, SNAP- and CLIP-tags have been widely

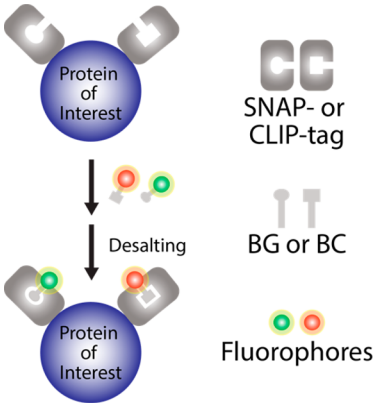

Figure 1. Schematic of orthogonal fluorophore labeling using the SNAP- and CLIP-tags fused to a protein of interest.

used as fusion partners to label proteins of interest for cellular imaging,[26,28−31] super-resolution microscopy,[28,32] FRET-based biosensors on cell surfaces,[33] in vitro protein conformational studies,[34] functionalizing nanoparticles,[35] cross-linking proteins,[36] and immobilizing a protein of interest on a surface.[37] These chemical tags have also been employed for fluorescent labeling in smFRET measurements;[38] however, a systematic evaluation of this labeling strategy is still lacking.

To fill this gap, we have chosen the SNAP-tag/CLIP-tag combination as a model system to systematically investigate the applicability of these comparatively large chemical tags as an alternative strategy to fluorescently labeling proteins for smFRET measurements. To evaluate the distance sensitivity of the system, we have fused a flexible 15 amino-acid peptide (15aa), 4 rigid polyproline (PP) peptides of different lengths (xPP, x = 6, 12, 20, and 24 prolines), and a calcium-sensitive protein (calcium-binding protein calmodulin, CaM) without additional linkers between the SNAP- and CLIP-tags and performed smFRET measurements on these constructs. We discuss our results in the context of previously published smFRET measurements on similar systems to evaluate the usability of the SNAP/CLIP-tag constructs.

EXPERIMENTAL METHODS

Materials. The Yellow Cameleon 3.6 vector (AAV-6P-SEW-YC3.6) coding for CaM and the M13 skeletal muscle myosin light-chain kinase (M13) peptide was a kind gift from Fritjof Helmchen (Addgene plasmid #31379).[39] All restriction enzymes and PCR reagents were purchased from Promega (Mannheim, Germany). SNAP-tag/CLIP-tag reactive dyes (SNAP-Cell TMR-Star (BG-TMR), SNAP-Surface Alexa Fluor 546 (BG-A546), and CLIP-Surface 647 (BC-DY647)) were purchased from New England Biolabs (Frankfurt am Main, Germany). The M13 peptide was purchased from Anaspec (Fremont, CA, USA) and used without further purification. All other reagents were purchased from Sigma-Aldrich (Munich, Germany).

Plasmid Preparation. The oligonucleotides coding for the PP peptides 6PP, 12PP, 20PP, and 24PP were purchased from Biomers (Ulm, Germany). The CaM gene without the M13 fragment was PCR amplified from the AAV-6P-SEW-YC3.6 vector. All genes were doubly digested (*Bam*HI and XhoI) and purified prior to subcloning into the pET51b-SNAP-Nbp2-CLIP (pET51b-S-Nbp2-C) vector in place of the Npb2 gene.

Protein Expression and Purification. The plasmids were transformed into chemically competent *E. coli* cells (BL21 (DE3)). The cells were plated on agar plates (75 μg/mL of Ampicillin) and incubated overnight at 37 °C. Single colonies were picked and grown overnight in 100 mL LB medium containing 75 μg/mL of Ampicillin. Twenty milliliters of the overnight culture was added to 3 L of 2× YT medium containing the antibiotic, grown at 37 °C at 160 rpm to OD_{600} = 0.6, induced by adding isopropyl-β-D-thio-galactoside (IPTG) to a final concentration of 1 mM and cultured overnight at 18 °C at 160 rpm. The cells were harvested by centrifugation at 5000*g* for 20 min. The pellet was resuspended in 15 mL of lysis buffer (50 mM sodium phosphate, 300 mM NaCl, pH 7.4, 1 mg/mL lysozyme, protease inhibitor cocktail, and 0.5% Triton X-100) and incubated for 30 min on ice. The cells were lysed using a probe sonicator (Bandelin, Berlin, Germany, 5% pulsation and 85% amplitude) for a total of 16 min with 5 min breaks every 2 min. The lysate was centrifuged at 20,000*g* for 20 min at 4 °C. The supernatant was loaded onto a His-tag column (6 mL profinity IMAC resin, Bio-Rad, Munich, Germany) attached to a Fast Protein Liquid Chromatography system (FPLC, ÄKTAexplorer 100, GE Healthcare, Freiburg, Germany). The column was pre-equilibrated with 5 column volumes of washing buffer (50 mM potassium phosphate, 20 mM imidazole, 300 mM NaCl, pH 7.5) at a flow rate of 2 mL/min. Proteins were eluted by running a linear gradient (0−100%) with the elution buffer (50 mM potassium phosphate, 500 mM imidazole, 300 mM NaCl pH 8.0) over 30 min at a flow rate of 2 mL/min. The purity of the protein aliquots was checked using precast 4−20% polyacrylamide SDS-PAGE gels (Bio-Rad). Pure fractions were pooled and concentrated using a Vivaspin 20 centrifugal concentrator (Thermo Fischer Scientific, Schwerte, Germany). The buffer of the concentrated protein sample was exchanged to labeling buffer (50 mM HEPES, pH 7.4) using a PD10 column (GE Healthcare). Glycerol was added to a final concentration of 25% (w/v) before protein stock aliquots were flash frozen with liquid nitrogen and stored at −80 °C.

Protein Labeling. The purified constructs (final concentration adjusted to 2.5 μM) were incubated with both donor (BG-A546 or BG-TMR) and acceptor (BC-DY647) dyes in a 1:2:2 molar ratio (protein:BG-dye:BC-dye) in labeling buffer supplemented with 1 mM dithiothreitol (DTT). After nutating the solution at room temperature for 1.5 h, free dye was removed by using a desalting column (NAP5, GE Healthcare or

DOI: 10.1021/acs.jpcb.5b03584
J. Phys. Chem. B XXXX, XXX, XXX−XXX

Micro Bio-Spin 6, Bio-Rad). If needed, the labeled protein was concentrated using a Vivaspin 6 centrifugal concentrator. Labeling efficiencies were determined spectroscopically. The presence of FRET was verified by ensemble fluorescence measurements.

Design of the Pentadecameric Peptide. The unstructured 15-amino acid polypeptide (GRLEVLFQGPKAFLE) was fused between the SNAP- and CLIP-tags (S-15aa-C) without additional linkers. The tags were labeled with BG-A546 and BC-DY647. The complete amino acid sequence of the S-15aa-C construct is given in the Supporting Information. To obtain the directly labeled polypeptide, two amino acids had to be substituted in the peptide sequence. The C-terminal Glu15 was replaced by Cys to allow conjugation of the Alexa Fluor 647 (A647) maleimide to the side chain thiol. Lys11 was replaced by an arginine to ensure the site-specific labeling of the Gly1 α-amino group with the Alexa Fluor 546 (A546) NHS ester. The doubly labeled pentadecameric peptide (A546-GRLEVLFQG-PRAFLC-A647, A546-15aa-A647) was synthesized and purified by PSL Peptide Specialty Laboratories GmbH (Heidelberg, Germany). The labeled peptide sample was first dissolved in dimethylformamide (DMF) and further diluted with storage buffer.

Ensemble FRET Measurements. Ensemble fluorescence emission measurements were performed at ambient temperature on a Fluorolog-3 spectrophotometer (HORIBA Jobin Yvon GmbH, Munich, Germany). The fluorescently labeled S-CaM-C (BG-TMR/BC-DY-647) sample was diluted to a final concentration of 25 nM in 25 mM Tris-HCl, 100 mM KCl, pH 7.5, supplemented with 1 μM to 133 mM $CaCl_2$. The samples were excited at 510 nm; emission spectra were recorded from 520−800 nm with the excitation and emission slits set to 5 nm. The emission spectrum of pure buffer (without $CaCl_2$) was used for background correction. All background-corrected spectra were normalized at the donor emission maximum (576 nm). The intensities at the acceptor peak (671 nm), which yield the FRET efficiency, were plotted as a function of Ca^{2+} concentration. The data were fitted using the Hill equation, $I_{671} = (I_{start} + (I_{end} - I_{start})([Ca^{2+}]^n/(K_d{}^n + [Ca^{2+}]^n))$, where I_{671} is the emission intensity at 671 nm after normalization at 576 nm, representing the relative population of folded CaM, I_{start} and I_{end} are the emission intensities at the start and end of the titration, respectively. $[Ca^{2+}]$ denotes the Ca^{2+} ion concentration, K_d is the equilibrium dissociation coefficient, and n is the Hill coefficient.

Single-Molecule FRET Measurements. All smFRET measurements on freely diffusing, fluorescently labeled SNAP-tag/CLIP-tag constructs were carried out on a custom-built confocal microscope based on a Zeiss Axiovert 135 TV. Details of the instrument can be found elsewhere.[40] In brief, the donor and acceptor dyes were excited by a 532 nm diode-pumped solid state laser (Excelsior 532-100-SLM-CDRH, Spectra Physics, Santa Clara, CA) at a power of 43 kW cm^{-2} and a 641 nm laser (DL 638−100, CrystaLaser, Reno, NV) at 110 kW cm^{-2}, respectively. The excitation was alternated between the two lasers by an acousto-optical tunable filter (AOTF, 106−225 MHz, Crystal Technology, Palo Alto, CA, USA) at a frequency of 10 kHz with a duty cycle of 70% for donor excitation and 30% for acceptor excitation.[41] Data collected within the first 5 μs after switching between excitation wavelengths were discarded to avoid temporal crosstalk. Out-of-focus light was removed by a pinhole (100 μm). The emitted light was separated into donor and acceptor channels by a dichroic beam splitter (640dcxr), filtered (HQ580/60 for the donor, 665LP for the acceptor), and detected by avalanche photodiode (APD) detectors (SPCM-AQR-14, PerkinElmer Optoelectronics, Wellesley, MA). All optical filters were purchased via AHF (Tübingen, Germany).

For single molecule measurements, the samples were diluted to 50−100 pM in the appropriate imaging buffer (15aa peptide and PP samples: 50 mM Tris-HCl, 300 mM NaCl, pH 7.4; CaM samples: 25 mM Tris-HCl, 100 mM KCl, pH 7.5), supplemented with 0.001% Tween 20 to reduce nonspecific adsorption of proteins onto the cover glass surface. One millimolar Trolox was added to suppress fluorophore blinking.[42] All buffers contained glucose oxidase (Sigma-Aldrich, from *Aspergillus niger*, 100 U/ml) and catalase (Calbiochem, Darmstadt, Germany, from bovine liver, 100 U/ml) in combination with 1% glucose (w/v) as the oxygen scavenging system.[43,44] The sample droplet (~30 μL) was deposited on a cover glass functionalized with polyethylene glycol.[45]

The collected fluorescence burst data were analyzed using custom analysis software written in Matlab 2014 (MathWorks, Natick, MA). All molecules with the donor emitting more than 50 photons within a single burst were selected for further data analysis. The donor and acceptor fluorescence intensities were used to calculate the FRET efficiencies (E_{FRET}) according to $E_{FRET} = I_a/(I_a + \gamma I_d)$, where I_a and I_d are the intensities of the acceptor and donor emissions, respectively. The parameter γ corrects for the different quantum yields of the two fluorophores and the different detection efficiencies of the setup. A γ value of 0.9 was found to be appropriate for all evaluations. To select molecules labeled with both a donor and an acceptor dye, stoichiometry filtering was applied.[41] The final FRET histograms were plotted and fitted using OriginPro 9.0 (OriginLab Co., Northampton, MA, USA).

The distance between the dyes, R, was estimated from the measured E_{FRET} values and the Förster radius, R_0, according to $R = R_0[(1 - E_{FRET})/E_{FRET}]^{1/6}$. The Förster radius, $R_0 = 0.211(\kappa^2\, Q_D\, n^{-4}\, J)^{1/6}$ (in Å), is specific for each dye pair and depends on the orientation factor (κ^2), the quantum yield of the donor dye (Q_D), the index of refraction of the solution (n), and the spectral overlap (J) between the donor emission spectrum and the acceptor excitation spectrum. Here, a value of 2/3 was used for orientation factor κ^2, assuming fast and unrestricted reorientation of the dyes.

RESULTS AND DISCUSSION

smFRET Study of a Pentadecameric Peptide. We have tested the applicability and sensitivity of the SNAP-tag/CLIP-tag FRET pair in smFRET experiments on various model constructs. In a first set of experiments, we quantified the effect of the tag size on the experimentally observed E_{FRET}. To this end, we labeled a 15-amino acid polypeptide with donor and acceptor dyes either directly (15aa, A546 (donor) and A647 (acceptor)) or via the SNAP-tag/CLIP-tags (S-15aa-C, BG-A546 (donor) and BC-DY647 (acceptor)). Figure 2 displays the E_{FRET} histograms of the two constructs obtained from single molecule measurements. Both histograms show a single distribution, indicative of a single population. This also shows that there is no transient interaction between SNAP-tag and CLIP-tag that could give rise to an additional subpopulation. Gaussian fits yielded center or average positions $\langle E_{FRET}\rangle = 0.81 \pm 0.01$ and $\langle E_{FRET}\rangle = 0.73 \pm 0.01$ for 15aa and S-15aa-C, respectively. As expected, $\langle E_{FRET}\rangle$ is shifted to a lower value for

DOI: 10.1021/acs.jpcb.5b03584
J. Phys. Chem. B XXXX, XXX, XXX−XXX

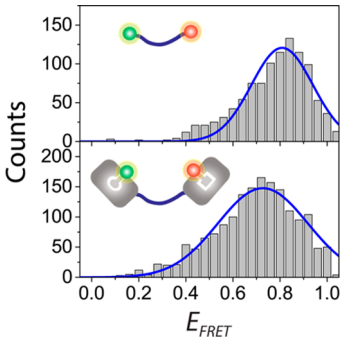

Figure 2. smFRET efficiency histograms of a directly labeled 15-aa peptide (top) and the S-15aa-C construct containing a SNAP- and CLIP-tag at the N- and C-termini, respectively (bottom).

the self-labeling tags due to the added distance between the dyes. The average distance between donor and acceptor dye, calculated from E_{FRET} and the respective Förster radii of the dye pairs (A546/A647: R_0 = 69 Å; A546/DY647: R_0 = 67 Å), increased from ~5.4 nm in the 15aa construct to ~5.7 nm in S-15aa-C. Using the Gaussian chain model, the average end-to-end distance (d) of a 15-aa peptide can be estimated as $d = b \times l^{0.5}$ = ~3.1 nm, where l indicates the number of peptide bonds; the effective bond length (b) was taken as 0.8 nm.[46] By including additional contributions from the linkers of the two dyes (i.e., from the nonaromatic, linear carbon chains connecting the functional groups and the actual chromophores), the estimated distance is in reasonable agreement with the physical dimensions of the labeled peptide. On the basis of the crystal structure of the SNAP-tag (PDB ID: 3KZY), the distances between the attachment site of the dye (i.e., the Cys145 thiol group) and the attachment site of the tag to the polypeptide (i.e., the N- and C-termini) are ~2.5 and 1.7 nm, respectively. This implies that the distance between donor and acceptor may increase by up to ~4 nm as compared to the directly labeled peptide. In addition, the dyes may protrude out of the binding site by up to ~2 nm because of their long linkers. The observed change of $\langle E_{FRET} \rangle$, however, indicates an average distance increase of only ~0.3 nm, which suggests that the SNAP- and CLIP-tags are not in the maximally extended conformation but possibly in a slightly tilted orientation toward each other.

Additionally, the width of the distribution recorded on S-15aa-C (2σ = 0.38 ± 0.02) was larger than that of the 15-aa construct (2σ = 0.26 ± 0.01). This increase (Figure 2) is most likely associated with the added flexibility of the S-15aa-C construct. The large tags and, therefore, the fluorophores as well, may tumble around their attachment points and sample a much larger volume than the directly attached dyes, which results in a wider distribution of possible E_{FRET} values. However, these fluctuations would have to occur on time scales slower than the experimental observation time of ~1 ms to not get averaged out. Photophysical effects, such as the quenching of dye molecules by tryptophan and tyrosine residues, may also contribute to the broadening of FRET efficiency distributions in smFRET experiments.

smFRET Studies of Polyprolines Fused between the SNAP- and CLIP-tags. Next, we fused PP peptides of different lengths between the two tags (S-xPP-C, x = 6, 12, 20, and 24 prolines) to test the distance sensitivity that can be resolved by smFRET measurements. PP is a rigid polypeptide that can serve as a molecular ruler.[47]

In Figure 3a and b, we have compiled the E_{FRET} histograms obtained from freely diffusing, doubly labeled S-xPP-C samples

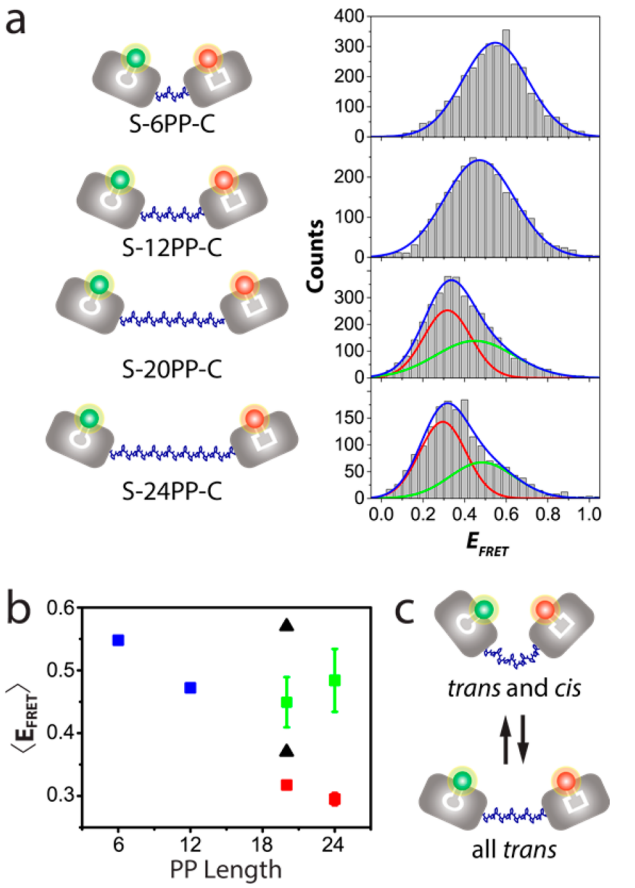

Figure 3. smFRET efficiency histograms of S-xPP-C constructs of different lengths. (a) Cartoon representations of the S-xPP-C constructs (x = 6, 12, 20, and 24) and the corresponding E_{FRET} histograms obtained from smFRET measurements. The data (gray bars) were fitted with one or a sum of two Gaussians (solid green and red lines: individual Gaussians; blue lines: single Gaussian or sum of the Gaussians) to obtain the peak positions of $\langle E_{FRET} \rangle$. (b) $\langle E_{FRET} \rangle$ (■) and corresponding errors of the fit for the S-xPP-C constructs. For comparison, $\langle E_{FRET} \rangle$ values from a two Gaussian fit of a directly labeled 20-PP sample (▲) are also included.[52] (c) In the PP peptide samples, proline residues are predominantly in the *trans* conformation (bottom), but there are also peptides with one or a few *cis* residues (top). Depending on the number of prolines in *cis* or *trans*, the average distance between the two terminal ends changes.

and their peak positions. These histograms reveal a systematic shift of $\langle E_{FRET} \rangle$ toward lower values with increasing length of the PP peptide. In the histograms of the 20PP and 24PP constructs, two subpopulations can be distinguished. The $\langle E_{FRET} \rangle$ values obtained from fitting the data in Figure 3a with Gaussian distributions are plotted in Figure 3b. The FRET histograms of 20PP and 24PP were fitted with two Gaussians. Whereas the distribution at the lower $\langle E_{FRET} \rangle$ shows a distinct dependence on the PP peptide length, the subpopulation at the higher $\langle E_{FRET} \rangle$ shows only a weak dependence as the length of the peptide increases. As a word of caution: although the two Gaussian fits describe the overall E_{FRET} histograms very well, the individual parameter areas, means, and widths should not be given much credence because the separation into the two distributions is fairly ambiguous.

DOI: 10.1021/acs.jpcb.5b03584
J. Phys. Chem. B XXXX, XXX, XXX−XXX

To explain our findings, we need to refer to the structural peculiarities of PPs. They predominantly form rather stiff type II *trans* helices with a pitch of 0.31 nm per residue, for which Schimmel and Flory have estimated a persistence length of 22 nm.[48] However, recent smFRET experiments and simulations have revealed shorter persistence lengths and substantial structural heterogeneity. In their smFRET studies on directly labeled PPs, Best et al.[49] observed much closer donor−acceptor distances than expected from the end-to-end distance of a rigid rod, which they explained by significant structural flexibility of the peptide. Watkins et al.[50] associated the heterogeneity to occasional *cis* residues interspersed in the *trans* repeats. In 2007, Doose et al.[51] probed PP dynamics using fluorescence quenching by photoinduced electron transfer and confirmed an inherent structural heterogeneity due to the presence of *cis* isomers. An NMR study further revealed that, for an aqueous solution, there is ∼2% probability for each proline to be in the *cis* conformation, which, for a 20PP peptide, implies that ∼30% of the molecules contain at least one *cis* isomer.[49,52] These isomers lead to pronounced kinks in the otherwise linear all-*trans* chain and, concomitantly, to higher mean FRET efficiencies (Figure 3c).[49,51−53] In our E_{FRET} histograms, the *cis* isomer-containing subpopulations give rise to the subtle shoulders in the histograms of the 20PP and 24PP constructs (Figure 3a). For the shorter PP constructs (6PP and 12PP), the probability of containing a *cis* isomer is smaller, and the expected difference in the $\langle E_{FRET}\rangle$ values due to *trans*−*cis* isomerization of a single proline is relatively small, such that those distributions can be described with single Gaussians. In addition, conformational heterogeneity is masked by the pronounced conformational flexibility of the large tags, causing a broadening of the FRET distributions. Overall, the subpopulation with the higher $\langle E_{FRET}\rangle$, which is expected to represent the population that contains *cis* isomer(s) and is therefore bent, shows only a slight decrease in the end-to-end distance as the length of the peptide increases.

Our smFRET data on S-20PP-C are in qualitative agreement with published data of a directly labeled 20PP construct[52] (Figure 3b). Both FRET histograms show two subpopulations with $\langle E_{FRET}\rangle \approx 0.37$ and $\langle E_{FRET}\rangle \approx 0.57$ for the directly labeled 20PP (▲ in Figure 3b) and $\langle E_{FRET}\rangle \approx 0.32$ and $\langle E_{FRET}\rangle \approx 0.45$ for S-20PP-C (■ in Figure 3b). As noted earlier for the 15-aa constructs, the increased distance between the dyes due to the larger SNAP-tag/CLIP-tag is again responsible for the lower $\langle E_{FRET}\rangle$ values of both subpopulations. Moreover, the S-20PP-C E_{FRET} histogram distributions are broader than those of the directly labeled construct.[52] The relative fractions of the two subpopulations, however, are comparable between the two labeling methods, indicating that the conformational state of the peptide is not significantly affected by the presence or nature of the tags.

In summary, our smFRET data indicate that distance variations on the order of four prolines (i.e., ∼1.2 nm) can be detected reliably when using the SNAP-tag/CLIP-tag system for FRET pair labeling.

Conformational Changes of Calmodulin. Finally, we tested the SNAP-tag/CLIP-tag system on a model protein that undergoes a large conformational change. Calmodulin (CALcium-MODULated protein, CaM) is a messenger protein of ∼17 kDa expressed in all eukaryotic cells. It consists of two approximately symmetric globular domains (the N- and C-domains) separated by a flexible linker region. Each domain contains two helix−loop−helix (EF-hand) motifs that each can bind a Ca^{2+} ion. The Ca^{2+}-free apo protein is essentially unfolded and highly flexible. Upon Ca^{2+} binding, CaM converts to a more rigid and stable holo conformation, which may occur independently for the two globular domains.[54] The holo form then binds to specific target sequences of regulatory proteins and alters their signaling properties. For example, it binds to myosin light chain kinase (MLCK) and, as a consequence, MLCK is activated and phosphorylates the myosin light chain, which allows myosin to hydrolyze ATP and go through the myosin cross-bridge cycle.[55] M13 is a synthetic peptide that has the same sequence as the CaM-binding domain of MLCK and, therefore, can mimic MLCK binding.[56]

We have fused CaM between the SNAP-tag/CLIP-tag pair and performed ensemble fluorescence measurements on the S-CaM-C construct to probe Ca^{2+} dependent conformational changes of the system. In Figure 4a, we have plotted ensemble fluorescence emission spectra with donor excitation at a wavelength of λ_{ex} = 510 nm under different solvent conditions. All spectra were normalized at the donor emission peak (576 nm). The emission spectrum in the presence of 1 mM EGTA showed a slightly lower acceptor emission at 671 nm (i.e., FRET signal) than the spectrum recorded at 0.5 μM Ca^{2+} (Figure 4a), indicating that there was only a low concentration of Ca^{2+} present in the buffer solution and that the majority of CaM molecules were in the unfolded, apo state. At 8.3 mM Ca^{2+}, the FRET signal was markedly increased, indicating formation of the holo protein. To determine the apparent Ca^{2+}

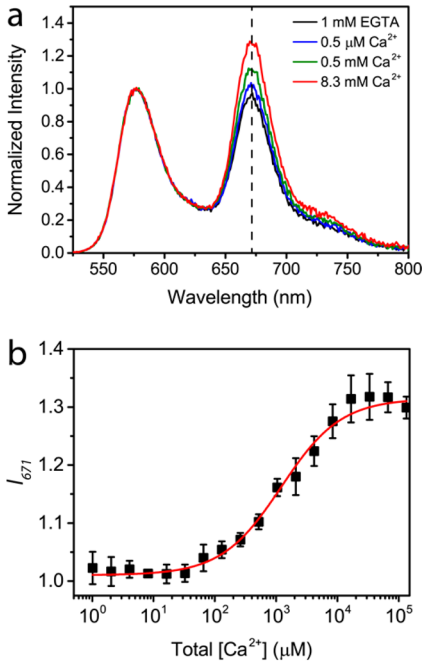

Figure 4. Bulk fluorescence measurements on S-CaM-C. (a) Ensemble fluorescence emission spectra of doubly labeled S-CaM-C (BG-TMR/BC-DY647) in 25 mM Tris-HCl, 100 mM KCl, pH 7.5, supplemented with 1 mM EGTA (black), 0.5 μM (blue), 0.5 mM (green), and 8.3 mM (red) Ca^{2+} ions. Spectra were normalized at 576 nm to show the relative change of the emission at 671 nm. (b) Normalized emission intensities at 671 nm, I_{671} (symbols), representing the relative CaM folded population, and the fit (line) using the Hill equation were plotted as a function of total Ca^{2+} ion concentration. Error bars represent the standard deviations obtained from three independent measurements.

DOI: 10.1021/acs.jpcb.5b03584
J. Phys. Chem. B XXXX, XXX, XXX−XXX

affinity, we recorded fluorescence emission spectra as a function of the Ca^{2+} ion concentration. Upon donor excitation at 510 nm, we observed a decrease of the donor emission at 576 nm and a corresponding increase of the acceptor emission at 671 nm. The Ca^{2+}-dependent changes in the emission at 671 nm are plotted in Figure 4b. The solid line represents the result of a fit with the Hill equation, yielding an average equilibrium dissociation constant of K_d = 1.2 ± 0.1 mM and a Hill coefficient of n = 0.89 ± 0.08. In site-specific binding studies of Ca^{2+} to the individual EF hand motifs of CaM, dissociation constants between 30 and ~1000 μM were found, which varyied for the different EF hand motifs studied and the buffer conditions.[57−59]

Overall, our ensemble FRET data confirm that the S-CaM-C construct folds in a Ca^{2+}-dependent manner but does not resolve the binding of Ca^{2+} ions to individual EF hand motifs. Apparently, conformational changes within these motifs do not affect the overall E_{FRET}. This result also shows that there is no significant interaction between SNAP-tag and CLIP-tag that could interfere with the assay. The slightly lower affinity that we have observed may arise from steric hindrance due to the presence of the large tags or reflect experimental differences (e.g., buffer composition, labeling position, organic dye and tryptophan fluorescence, or NMR and fluorescence), in particular, the recorded parameters used to determine the conformational changes. Careful control experiments are advised when applying this approach to different protein systems.

To resolve individual conformational substates of the S-CaM-C construct, we performed smFRET measurements under different buffer conditions. Figure 5a shows representative E_{FRET} histograms of S-CaM-C in CaM imaging buffer supplemented with 10 mM EGTA (top panel), 1 mM Ca^{2+} (middle), and 10 μM M13/1 mM Ca^{2+} (bottom). In the presence of EGTA, the E_{FRET} distribution is well described by a single Gaussian population with $\langle E_{FRET}\rangle$ = 0.40 ± 0.01. Comparison of the three histograms shows that this is the lowest average FRET, suggesting that the CaM domain is in the Ca^{2+}-free, highly dynamic apo conformation. In the presence of Ca^{2+} ions, the E_{FRET} distribution is shifted to higher values and is significantly broader. The data can be described satisfactorily by two Gaussian distributions, one at $\langle E_{FRET}\rangle$ = 0.40 (fixed to the value without Ca^{2+}) and a second at $\langle E_{FRET}\rangle$ = 0.65 ± 0.02 with fractional populations of 57 and 43%, respectively. From these data, we have computed an overall weighted average $\langle E_{FRET}\rangle$ = 0.51 ± 0.05, which indicates a more compact conformation and, thus, increased folding of the protein. Upon addition of the M13 peptide, the fraction of the high E_{FRET} subpopulation ($\langle E_{FRET}\rangle$ = 0.65 ± 0.01) significantly increased to 72%, causing a shift of the overall average $\langle E_{FRET}\rangle$ to 0.58 ± 0.06. This result clearly indicates the stabilizing effect of the M13 peptide on the folded state. However, under both 1 mM Ca^{2+} and M13/1 mM Ca^{2+} conditions, the broad E_{FRET} distribution did not permit us to assess any further heterogeneity due to the folding of the individual EF hand motifs.

In Figure 5b, we compare our $\langle E_{FRET}\rangle$ values with those obtained on CaM directly and site-specifically labeled with a Cy3/Cy5 dye pair (Förster radius R_0 = 54 Å) at positions 34 and 113 by using unnatural amino acids.[9] For both constructs, $\langle E_{FRET}\rangle$ clearly increases upon the addition of M13/Ca^{2+}; however, the similarity stops there. For the directly labeled CaM, no significant difference was observed in the peak

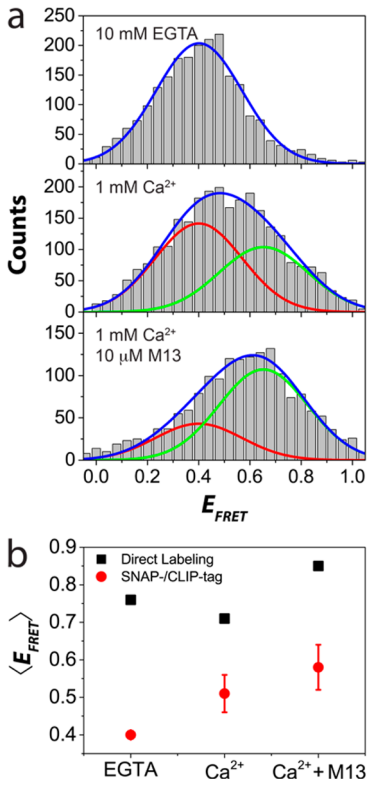

Figure 5. Results from smFRET measurements on the S-CaM-C construct. (a) smFRET histograms of S-CaM-C with 10 mM EGTA, 1 mM Ca^{2+}, and 10 μM M13/1 mM Ca^{2+}. The data (gray bars) were fitted with one or a sum of two Gaussians (represented by red and green lines). The peak position and the width of the distribution in the presence of EGTA was fixed (red line) to obtain the second Gaussian fit (green). (b) Comparison of the overall $\langle E_{FRET}\rangle$ determined from the distributions in panel (a) and from measurements of directly labeled CaM.[9] Error bars represent the error of the fit.

position for the measurements with or without Ca^{2+} ions present in the buffer. In that study, the effect of Ca^{2+} ions was only apparent from the widths of the distributions with the sample in EGTA showing a narrower width parameter (σ) of the fitted Gaussian (σ_{EGTA} = 0.12; $\sigma_{Ca^{2+}}$ = 0.20). Apparently, the labeling sites within the protein were not chosen such as to reveal the different conformational states of the system through a change in $\langle E_{FRET}\rangle$. This illustrates once again that smFRET measurements are exquisitely dependent on the proper choice of the fluorophore attachment sites. Moreover, in all directly labeled samples, only a single E_{FRET} distribution was observed. By contrast, the S-CaM-C histograms revealed conformational heterogeneity, indicating that both folded and unfolded CaM species exist in the presence of calcium and M13. This result is supported by an optical tweezer study in which dynamic folding and unfolding of CaM was observed even in the presence of Ca^{2+} ions.[54] Apparently, here and likely also in other studies, the use of enzymatic tags offers a way to add the necessary distance between the FRET labels to uncover otherwise hidden conformations of a protein being studied.

CONCLUSIONS

In summary, we have presented a variety of proof-of-principle smFRET experiments using various SNAP-tag and CLIP-tag labeled constructs, showing successfully employment of these relatively large chemical tags. Similar results are expected with

DOI: 10.1021/acs.jpcb.5b03584
J. Phys. Chem. B XXXX, XXX, XXX−XXX

other chemical tags, such as the Halo- and TMP-tags, due to their comparable size. The obvious advantage of the system is the possibility to quickly, orthogonally, and specifically attach a FRET dye pair to even larger proteins. The smFRET measurement on the S-15aa-C construct showed that the SNAP-tag/CLIP-tag FRET system also comes with a caveat. In comparison with the directly labeled 15aa peptide, we found a decrease in the FRET efficiency as well as a broadening of the FRET distributions due to the added displacement of the dyes and the flexibility of the tags. Our study of a series of PP constructs indicates that even a small difference in the interdye distance corresponding to four prolines can be detected. The functionality of the protein of interest is of concern whenever a dye is attached or a fusion protein is added. To this end, we have also tested the SNAP-tag/CLIP-tag system on CaM, which undergoes a large conformational change in the presence of calcium ions. Indeed, the SNAP-tag/CLIP-tag labeled construct performed the expected conformational changes for CaM alone. To our surprise, the change in $\langle E_{FRET} \rangle$ upon variation of the buffer conditions was more pronounced than for directly labeled CaM. This result shows that the additional distance provided by the chemical tags can be beneficial to reveal conformational substates that are otherwise hidden because of a shorter interdye distance. We have limited our study to the SNAP-tag/CLIP-tag fused at the N- and C-terminal ends of the peptide or protein. In larger multidomain protein systems, internal labeling may also be applicable and perhaps easier to implement. This study was carried out strictly by using in vitro techniques; however, with proper control experiments, this method may become a valuable tool for in vivo live cell measurements to probe large conformational changes as well as for advanced in vitro single molecule measurements using cell extracts to study proteins expressed in native environments.[60−62]

■ ASSOCIATED CONTENT

Supporting Information

Amino acid sequences of all constructs used in the current study. The Supporting Information is available free of charge on the ACS Publications website at DOI: 10.1021/acs.jpcb.5b03584.

■ AUTHOR INFORMATION

Corresponding Author

*E-mail: uli@uiuc.edu.

Present Address

[¶]N.A.: Center for Plant Molecular Biology, University of Tübingen, Auf der Morgenstelle 32, 72076 Tübingen, Germany.

Author Contributions

[‡]Y.I. and N.A. contributed equally.

Notes

The authors declare no competing financial interest.

■ ACKNOWLEDGMENTS

This work was supported by contract research within the research program "Methoden für die Lebenswissenschaften" of the Baden-Württemberg Stiftung and by the Karlsruhe School of Optics and Photonics (KSOP), Karlsruhe Institute of Technology (KIT) in the context of the Helmholtz STN program and Deutsche Forschungsgemeinschaft (DFG) Grant GRK 2039. The authors thank Dr. Judith Müller (Ulm University) for providing plasmid pET51b-S-Nbp2-C.

■ REFERENCES

(1) Förster, T. Energiewanderung und Fluoreszenz. *Naturwissenschaften* **1946**, *33*, 166−175.

(2) Förster, T. Zwischenmolekulare Energiewanderung und Fluoreszenz. *Ann. Phys.* **1948**, *2*, 55−75.

(3) Stryer, L.; Haugland, R. P. Energy Transfer: A Spectroscopic Ruler. *Proc. Natl. Acad. Sci. U.S.A.* **1967**, *58*, 719−726.

(4) Ha, T.; Tinnefeld, P. Photophysics of Fluorescent Probes for Single-Molecule Biophysics and Super-Resolution Imaging. *Annu. Rev. Phys. Chem.* **2012**, *63*, 595−617.

(5) Joo, C.; Balci, H.; Ishitsuka, Y.; Buranachai, C.; Ha, T. Advances in Single-Molecule Fluorescence Methods for Molecular Biology. *Annu. Rev. Biochem.* **2008**, *77*, 51−76.

(6) Li, G. W.; Xie, X. S. Central Dogma at the Single-Molecule Level in Living Cells. *Nature* **2011**, *475*, 308−315.

(7) Kuzmenkina, E. V.; Heyes, C. D.; Nienhaus, G. U. Single-Molecule FRET Study of Denaturant Induced Unfolding of RNase H. *J. Mol. Biol.* **2006**, *357*, 313−324.

(8) Puljung, M. C.; Zagotta, W. N. Labeling of Specific Cysteines in Proteins Using Reversible Metal Protection. *Biophys. J.* **2011**, *100*, 2513−2521.

(9) Kim, J.; Seo, M. H.; Lee, S.; Cho, K.; Yang, A.; Woo, K.; Kim, H. S.; Park, H. S. Simple and Efficient Strategy for Site-Specific Dual Labeling of Proteins for Single-Molecule Fluorescence Resonance Energy Transfer Analysis. *Anal. Chem.* **2013**, *85*, 1468−1474.

(10) Liu, C. C.; Schultz, P. G. Adding New Chemistries to the Genetic Code. *Annu. Rev. Biochem.* **2010**, *79*, 413−444.

(11) Seo, M. H.; Lee, T. S.; Kim, E.; Cho, Y. L.; Park, H. S.; Yoon, T. Y.; Kim, H. S. Efficient Single-Molecule Fluorescence Resonance Energy Transfer Analysis by Site-Specific Dual-Labeling of Protein Using an Unnatural Amino Acid. *Anal. Chem.* **2011**, *83*, 8849−8854.

(12) Wang, L.; Brock, A.; Herberich, B.; Schultz, P. G. Expanding the Genetic Code of *Escherichia coli*. *Science* **2001**, *292*, 498−500.

(13) Uchinomiya, S. H.; Nonaka, H.; Fujishima, S. H.; Tsukiji, S.; Ojida, A.; Hamachi, I. Site-Specific Covalent Labeling of His-Tag Fused Proteins with a Reactive Ni(II)-NTA Probe. *Chem. Commun. (Cambridge, U.K.)* **2009**, 5880−5882.

(14) Carrico, I. S.; Carlson, B. L.; Bertozzi, C. R. Introducing Genetically Encoded Aldehydes into Proteins. *Nat. Chem. Biol.* **2007**, *3*, 321−322.

(15) Shi, X.; Jung, Y.; Lin, L. J.; Liu, C.; Wu, C.; Cann, I. K.; Ha, T. Quantitative Fluorescence Labeling of Aldehyde-Tagged Proteins for Single-Molecule Imaging. *Nat. Methods* **2012**, *9*, 499−503.

(16) Griffin, B. A.; Adams, S. R.; Tsien, R. Y. Specific Covalent Labeling of Recombinant Protein Molecules inside Live Cells. *Science* **1998**, *281*, 269−272.

(17) Jager, M.; Nir, E.; Weiss, S. Site-Specific Labeling of Proteins for Single-Molecule FRET by Combining Chemical and Enzymatic Modification. *Protein Sci.* **2006**, *15*, 640−646.

(18) Yano, Y.; Yano, A.; Oishi, S.; Sugimoto, Y.; Tsujimoto, G.; Fujii, N.; Matsuzaki, K. Coiled-Coil Tag-Probe System for Quick Labeling of Membrane Receptors in Living Cell. *ACS Chem. Biol.* **2008**, *3*, 341−345.

(19) Muralidharan, V.; Muir, T. W. Protein Ligation: An Enabling Technology for the Biophysical Analysis of Proteins. *Nat. Methods* **2006**, *3*, 429−438.

(20) Vila-Perello, M.; Liu, Z.; Shah, N. H.; Willis, J. A.; Idoyaga, J.; Muir, T. W. Streamlined Expressed Protein Ligation Using Split Inteins. *J. Am. Chem. Soc.* **2013**, *135*, 286−292.

(21) Parthasarathy, R.; Subramanian, S.; Boder, E. T. Sortase a as a Novel Molecular "Stapler" for Sequence-Specific Protein Conjugation. *Bioconjugate Chem.* **2007**, *18*, 469−476.

(22) Popp, M. W.; Antos, J. M.; Grotenbreg, G. M.; Spooner, E.; Ploegh, H. L. Sortagging: A Versatile Method for Protein Labeling. *Nat. Chem. Biol.* **2007**, *3*, 707−708.

DOI: 10.1021/acs.jpcb.5b03584
J. Phys. Chem. B XXXX, XXX, XXX−XXX

(23) So, M. K.; Yao, H.; Rao, J. HaloTag Protein-Mediated Specific Labeling of Living Cells with Quantum Dots. *Biochem. Biophys. Res. Commun.* **2008**, *374*, 419−423.
(24) Calloway, N. T.; Choob, M.; Sanz, A.; Sheetz, M. P.; Miller, L. W.; Cornish, V. W. Optimized Fluorescent Trimethoprim Derivatives for in Vivo Protein Labeling. *ChemBioChem* **2007**, *8*, 767−774.
(25) Miller, L. W.; Cai, Y.; Sheetz, M. P.; Cornish, V. W. In Vivo Protein Labeling with Trimethoprim Conjugates: A Flexible Chemical Tag. *Nat. Methods* **2005**, *2*, 255−257.
(26) Gautier, A.; Juillerat, A.; Heinis, C.; Correa, I. R.; Kindermann, M.; Beaufils, F.; Johnsson, K. An Engineered Protein Tag for Multiprotein Labeling in Living Cells. *Chem. Biol.* **2008**, *15*, 128−136.
(27) Keppler, A.; Gendreizig, S.; Gronemeyer, T.; Pick, H.; Vogel, H.; Johnsson, K. A General Method for the Covalent Labeling of Fusion Proteins with Small Molecules in Vivo. *Nat. Biotechnol.* **2003**, *21*, 86−89.
(28) Klein, T.; Loschberger, A.; Proppert, S.; Wolter, S.; van de Linde, S.; Sauer, M. Live-Cell dStorm with Snap-Tag Fusion Proteins. *Nat. Methods* **2011**, *8*, 7−9.
(29) Albizu, L.; Cottet, M.; Kralikova, M.; Stoev, S.; Seyer, R.; Brabet, I.; Roux, T.; Bazin, H.; Bourrier, E.; Lamarque, L.; et al. Time-Resolved FRET between GPCR Ligands Reveals Oligomers in Native Tissues. *Nat. Chem. Biol.* **2010**, *6*, 587−594.
(30) Bosch, P. J.; Correa, I. R., Jr.; Sonntag, M. H.; Ibach, J.; Brunsveld, L.; Kanger, J. S.; Subramaniam, V. Evaluation of Fluorophores to Label Snap-Tag Fused Proteins for Multicolor Single-Molecule Tracking Microscopy in Live Cells. *Biophys. J.* **2014**, *107*, 803−814.
(31) Grimm, J. B.; English, B. P.; Chen, J.; Slaughter, J. P.; Zhang, Z.; Revyakin, A.; Patel, R.; Macklin, J. J.; Normanno, D.; Singer, R. H.; et al. A General Method to Improve Fluorophores for Live-Cell and Single-Molecule Microscopy. *Nat. Methods* **2015**, *12*, 244−250.
(32) Jones, S. A.; Shim, S. H.; He, J.; Zhuang, X. Fast, Three-Dimensional Super-Resolution Imaging of Live Cells. *Nat. Methods* **2011**, *8*, 499−508.
(33) Brun, M. A.; Tan, K.-T.; Nakata, E.; Hinner, M. J.; Johnsson, K. Semisynthetic Fluorescent Sensor Proteins Based on Self-Labeling Protein Tags. *J. Am. Chem. Soc.* **2009**, *131*, 5873−5884.
(34) Tyagi, S.; VanDelinder, V.; Banterle, N.; Fuertes, G.; Milles, S.; Agez, M.; Lemke, E. A. Continuous Throughput and Long-Term Observation of Single-Molecule FRET without Immobilization. *Nat. Methods* **2014**, *11*, 297−350.
(35) Kampmeier, F.; Ribbert, M.; Nachreiner, T.; Dembski, S.; Beaufils, F.; Brecht, A.; Barth, S. Site-Specific, Covalent Labeling of Recombinant Antibody Fragments Via Fusion to an Engineered Version of 6-O-Alkylguanine DNA Alkyltransferase. *Bioconjugate Chem.* **2009**, *20*, 1010−1015.
(36) Gautier, A.; Nakata, E.; Lukinavicius, G.; Tan, K. T.; Johnsson, K. Selective Cross-Linking of Interacting Proteins Using Self-Labeling Tags. *J. Am. Chem. Soc.* **2009**, *131*, 17954−17962.
(37) Engin, S.; Fichtner, D.; Wedlich, D.; Fruk, L. Snap-Tag as a Tool for Surface Immobilization. *Curr. Pharm. Des.* **2013**, *19*, 5443−5448.
(38) Tyagi, S.; VanDelinder, V.; Banterle, N.; Fuertes, G.; Milles, S.; Agez, M.; Lemke, E. A. Continuous Throughput and Long-Term Observation of Single-Molecule FRET without Immobilization. *Nat. Methods* **2014**, *11*, 297−300.
(39) Minderer, M.; Liu, W.; Sumanovski, L. T.; Kugler, S.; Helmchen, F.; Margolis, D. J. Chronic Imaging of Cortical Sensory Map Dynamics Using a Genetically Encoded Calcium Indicator. *J. Physiol.* **2012**, *590*, 99−107.
(40) Heyes, C. D.; Kobitski, A. Y.; Amirgoulova, E. V.; Nienhaus, G. U. Biocompatible Surfaces for Specific Tethering of Individual Protein Molecules. *J. Phys. Chem. B* **2004**, *108*, 13387−13394.
(41) Kapanidis, A. N.; Lee, N. K.; Laurence, T. A.; Doose, S.; Margeat, E.; Weiss, S. Fluorescence-Aided Molecule Sorting: Analysis of Structure and Interactions by Alternating-Laser Excitation of Single Molecules. *Proc. Natl. Acad. Sci. U.S.A.* **2004**, *101*, 8936−8941.
(42) Rasnik, I.; McKinney, S. A.; Ha, T. Nonblinking and Long-Lasting Single-Molecule Fluorescence Imaging. *Nat. Methods* **2006**, *3*, 891−893.
(43) Myong, S.; Cui, S.; Cornish, P. V.; Kirchhofer, A.; Gack, M. U.; Jung, J. U.; Hopfner, K. P.; Ha, T. Cytosolic Viral Sensor RIG-I Is a 5′-Triphosphate-Dependent Translocase on Double-Stranded RNA. *Science* **2009**, *323*, 1070−1074.
(44) Shi, X.; Lim, J.; Ha, T. Acidification of the Oxygen Scavenging System in Single-Molecule Fluorescence Studies: In Situ Sensing with a Ratiometric Dual-Emission Probe. *Anal. Chem.* **2010**, *82*, 6132−6138.
(45) Diao, J.; Ishitsuka, Y.; Lee, H.; Joo, C.; Su, Z.; Syed, S.; Shin, Y. K.; Yoon, T. Y.; Ha, T. A Single Vesicle-Vesicle Fusion Assay for in Vitro Studies of Snares and Accessory Proteins. *Nat. Protoc.* **2012**, *7*, 921−934.
(46) Zhou, H. X. A Gaussian-Chain Model for Treating Residual Charge-Charge Interactions in the Unfolded State of Proteins. *Proc. Natl. Acad. Sci. U.S.A.* **2002**, *99*, 3569−3574.
(47) Schuler, B.; Lipman, E. A.; Steinbach, P. J.; Kumke, M.; Eaton, W. A. Polyproline and the "Spectroscopic Ruler" Revisited with Single-Molecule Fluorescence. *Proc. Natl. Acad. Sci. U.S.A.* **2005**, *102*, 2754−2759.
(48) Schimmel, P. R.; Flory, P. J. Conformational Energy and Configurational Statistics of Poly-L-Proline. *Proc. Natl. Acad. Sci. U.S.A.* **1967**, *58*, 52−59.
(49) Best, R. B.; Merchant, K. A.; Gopich, I. V.; Schuler, B.; Bax, A.; Eaton, W. A. Effect of Flexibility and Cis Residues in Single-Molecule FRET Studies of Polyproline. *Proc. Natl. Acad. Sci. U.S.A.* **2007**, *104*, 18964−18969.
(50) Watkins, L. P.; Chang, H.; Yang, H. Quantitative Single-Molecule Conformational Distributions: A Case Study with Poly-(L-Proline). *J. Phys. Chem. A* **2006**, *110*, 5191−5203.
(51) Doose, S.; Neuweiler, H.; Barsch, H.; Sauer, M. Probing Polyproline Structure and Dynamics by Photoinduced Electron Transfer Provides Evidence for Deviations from a Regular Polyproline Type II Helix. *Proc. Natl. Acad. Sci. U.S.A.* **2007**, *104*, 17400−17405.
(52) Hoefling, M.; Lima, N.; Haenni, D.; Seidel, C. A.; Schuler, B.; Grubmüller, H. Structural Heterogeneity and Quantitative FRET Efficiency Distributions of Polyprolines through a Hybrid Atomistic Simulation and Monte Carlo Approach. *PLoS One* **2011**, *6*, e19791.
(53) Schuler, B.; Lipman, E. A.; Eaton, W. A. Probing the Free-Energy Surface for Protein Folding with Single-Molecule Fluorescence Spectroscopy. *Nature* **2002**, *419*, 743−747.
(54) Stigler, J.; Ziegler, F.; Gieseke, A.; Gebhardt, J. C.; Rief, M. The Complex Folding Network of Single Calmodulin Molecules. *Science* **2011**, *334*, 512−516.
(55) Gao, Y.; Ye, L. H.; Kishi, H.; Okagaki, T.; Samizo, K.; Nakamura, A.; Kohama, K. Myosin Light Chain Kinase as a Multifunctional Regulatory Protein of Smooth Muscle Contraction. *IUBMB Life* **2001**, *51*, 337−344.
(56) Blumenthal, D. K.; Takio, K.; Edelman, A. M.; Charbonneau, H.; Titani, K.; Walsh, K. A.; Krebs, E. G. Identification of the Calmodulin-Binding Domain of Skeletal Muscle Myosin Light Chain Kinase. *Proc. Natl. Acad. Sci. U.S.A.* **1985**, *82*, 3187−3191.
(57) Junker, J. P.; Ziegler, F.; Rief, M. Ligand-Dependent Equilibrium Fluctuations of Single Calmodulin Molecules. *Science* **2009**, *323*, 633−637.
(58) Lakowski, T. M.; Lee, G. M.; Okon, M.; Reid, R. E.; McIntosh, L. P. Calcium-Induced Folding of a Fragment of Calmodulin Composed of EF-Hands 2 and 3. *Protein Sci.* **2007**, *16*, 1119−1132.
(59) Ye, Y.; Lee, H. W.; Yang, W.; Shealy, S.; Yang, J. J. Probing Site-Specific Calmodulin Calcium and Lanthanide Affinity by Grafting. *J. Am. Chem. Soc.* **2005**, *127*, 3743−3750.
(60) Hoskins, A. A.; Friedman, L. J.; Gallagher, S. S.; Crawford, D. J.; Anderson, E. G.; Wombacher, R.; Ramirez, N.; Cornish, V. W.; Gelles, J.; Moore, M. J. Ordered and Dynamic Assembly of Single Spliceosomes. *Science* **2011**, *331*, 1289−1295.
(61) Jain, A.; Liu, R.; Ramani, B.; Arauz, E.; Ishitsuka, Y.; Ragunathan, K.; Park, J.; Chen, J.; Xiang, Y. K.; Ha, T. Probing

DOI: 10.1021/acs.jpcb.5b03584
J. Phys. Chem. B XXXX, XXX, XXX−XXX

Cellular Protein Complexes Using Single-Molecule Pull-Down. *Nature* **2011**, *473*, 484−488.
(62) Joo, C.; Fareh, M.; Kim, V. N. Bringing Single-Molecule Spectroscopy to Macromolecular Protein Complexes. *Trends Biochem. Sci.* **2013**, *38*, 30−37.

DOI: 10.1021/acs.jpcb.5b03584
J. Phys. Chem. B XXXX, XXX, XXX−XXX